Optimal Siting of UPFC on a Transmission Line with the Aim of Better Damping of Low Frequency Oscillations

Reza Gholizadeh-Roshanagh[*], **Behrouz Mohammadzadeh**[**,†], and **Sajad Najafi-Ravadanegh**[*], Non-members

ABSTRACT

Low frequency oscillations may cause blackouts. Power system operators are increasingly facing instability problems due to the fact that the current system is much more loaded than before. Tuning the lead-lag controllers, as power system stabilizers (PSS) or FACTS-based supplementary stabilizers, is a well-established method to enhance the damping capability of power systems. In this paper we propose a technique to optimally locate the place of unified power flow controller (UPFC) on a transmission line considering low frequency oscillation (LFO) damping. A lead-lag compensator is designed for UPFC based on imperialist competitive algorithm (ICA). The proposed method is applied to a single machine infinite bus system equipped with UPFC and the results obtained show its superiority.

Keywords: Imperialist Competitive Algorithm (ICA), Low Frequency Oscillation (LFO), Siting of UPFC, Supplementary Controller.

1. NOMENCLATURE

a	objective function parameter
BT	boosting transformer
C_{dc}	DC capacitor
COA	cuckoo optimization algorithm
D	machine damping coefficient
DC	direct current
E_{fd}	equivalent excitation voltage
$E_q^{'}$	internal voltage behind transient reactance
ET	excitation transformer
f	frequency
FACTS	flexible AC transmission systems
GA	genetic algorithm
GTO	gate turn off thyristor
i_B	boosting current
ICA	imperialist competitive algorithm
i_E	excitation current
J	objective function
k	proportional gain of the controller
k_S	proportional gain of the SSSC controller
LFO	lower frequency oscillations
M	machine inertia coefficient
m_B	boosting amplitude modulation ratio
m_E	excitation amplitude modulation ratio
P_e	active power
P_m	mechanical input power
PMU	phasor measurement unit
PSO	particle swarm optimization
PSS	power system stabilizer
Q_e	reactive power
SMIB	single machine infinite bus
SSSC	static synchronous series compensator
STATCOM	static synchronous compensator
SVD	singular value decomposition
T_1	lead time constant of controller
T_2	lag time constant of controller
T_3	lead time constant of controller
T_4	lag time constant of controller
$T_{d0}^{'}$	time constant of excitation circuit
T_S	time constant of the SSSC controller
T_w	washout time constant
UPFC	unified power flow controller
v	terminal voltage
v_b	infinite bus voltage
v_{Bt}	boosting voltage
v_{Et}	excitation voltage
v_{ref}	reference voltage
VSC	voltage source converter
x_B	boosting transformer reactance
x_d	d-axis reactance
$x_d^{'}$	d-axis transient reactance
x_E	excitation transformer reactance
x_q	q-axis reactance
x_{sb}	transmission line reactance after UPFC
x_{tE}	transformer reactance
x_{ts}	transmission line reactance before UPFC

Manuscript received on June 27, 2015 ; revised on January 29, 2016.

* The authors are with Smart Distribution Grid Research Lab, Department of Electrical Engineering, Azarbaijan Shahid Madani University, Tabriz, Iran,
E-mails: rezagholizadeh@azaruniv.edu; s.najafi@azaruniv.edu.
** The author is with the Young Researchers and Elite Club, Germi Branch, Islamic Azad University, Germi, Iran.
† The author is with the Department of Electrical Engineering, Payame Noor University, PO Box 19395-3697 Tehran , Iran.

δ	rotor angle
δ_B	boosting phase angle
δ_E	excitation phase angle
ΔP_e	electrical power deviation
Δv_{dc}	DC voltage deviation
$\Delta\delta$	rotor angle deviation
$\Delta\omega$	rotor speed deviation
ζ	damping ratio
σ	damping factor
ω	rotor speed
ω_b	base rotor speed

2. INTRODUCTION

As electric power demand grows rapidly and generation is restricted with the limited availability of resources and the strict environmental constraints, power transmission lines are today working near their stability limits. Since the development of interconnected large electric power systems, there have been spontaneous system oscillations at very low frequencies in the order of 1 Hz or below. If not well damped, these oscillations may keep growing in magnitude and may result in loss of synchronism [1]. Power system stabilizers (PSSs) have been extensively used to increase the system damping for low frequency oscillations. However, power system operators experienced problems in using PSSs. Some of these were, incapability in damping inter-area modes of oscillations, great variations in the voltage profile under severe disturbances and possibility of leading power factor operation therefore loss of system stability [2].

The problems of PSSs can be avoided using Flexible AC transmission systems (FACTS). FACTS have gained a great interest during the last few years, due to recent advances in power electronics. FACTS devices have been mainly used for solving various power system steady state control problems such as voltage regulation, power flow control, and transfer capability enhancement. As supplementary functions, damping the inter-area modes and enhancing power system stability using FACTS controllers have been extensively studied and investigated [2].

Nowdays, FACTS devices have been proved to be one of the most effective ways to improve power system operation controllability and power transfer limits. Unified power flow controller (UPFC) is the most versatile second generation FACTS device.

UPFC is a FACTS device that combine Static Compensator (STATCOM) and Static Synchronous Series Compensator (SSSC). Because of that combination, UPFC acquires both advantages of STATCOM and SSSC, and is able to perform many functions: voltage control, transient stability improvement, and oscillation damping [3].

Investigations on the UPFC main control effects show that the UPFC can improve system transient stability and enhance the system transfer limit as well. Nabavi-Niaki and Iravani [4] developed a steady-state model, a small-signal linearized dynamic model, and a state-space large-signal model of a UPFC. Wang has presented a modified linearized Phillips-Heffron model of a power system installed with a UPFC [5,6]. Wang has addressed the basic issues pertaining to the design of UPFC damping controllers, i.e., the selection of robust operating conditions for designing damping controllers; and the choice of parameters of the UPFC (such as m_E, m_B, δ_E, and δ_B) to be modulated to achieve the desired damping. But Wang has not presented a systematic approach to design the damping controllers.

Recently, researchers have proposed different problem formulations and different optimization methods to design UPFC-based supplementary controller for power system oscillation damping such as PSO, GA, ICA, COA, Linear Matrix Inequality (LMI) and Adaptive Neuro-Fuzzy Inference System (ANFIS) [1, 7-12]. However all of them have studied damping capability of UPFC, installed on the sending bus of a transmission line. it may be due to the availability of machines' signal e.g. rotor speed deviation. Today, in the presence of smart grid and the use of recent technologies like phasor measurement units (PMU), system operators can place the FACTS devices anywhere without considering the available input signals of supplementary controllers.

According to M. A. Abido [2], it is the objective of installation that determines the location of FACTS devices. He categorized the proposed objectives as increasing system loadability [13-17], minimizing the total generation cost [18], and enhancing voltage stability [19].

In this work, we suggest a method to determine the suitable location of UPFC on a transmission line, in order to best damping of low frequency oscillations. In order to show the significance of the proposed method, it is used and compared with a UPFC supplementary controller, designed using an evolutionary technique, imperialist competitive algorithm (ICA) [10, 20]. For this purpose eigenvalue analysis and time domain simulations are performed and discussed.

3. REPRESENTATION OF CASE STUDY SYSTEM WITH UPFC

The single machine infinite bus (SMIB) power system shown in Fig. 1 is used in this study. The UPFC is installed on the transmission line. The UPFC includes an excitation transformer (ET), a boosting transformer (BT), two three-phase GTO based voltage source converters (VSCs), and a DC link capacitor. The four input control signals to the UPFC are m_E, m_B, δ_E, and δ_B, where m_E is the excitation amplitude modulation ratio, m_B is the boosting amplitude modulation ratio, δ_E is the excitation phase angle and δ_B is the boosting phase angle. In Fig.1, x_{tE} represents the reactance of the transformer and

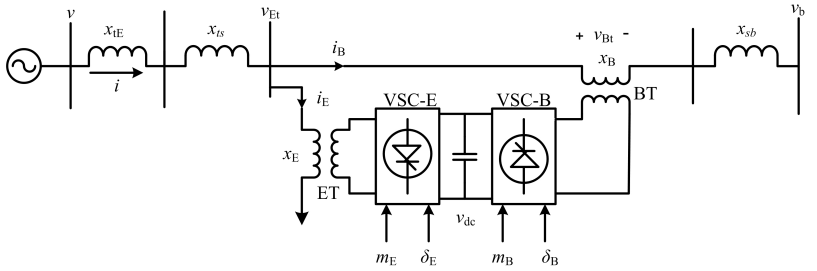

Fig.1: *Single machine infinite bus system equipped with UPFC.*

the x_{ts} and x_{sb} are the transmission line reactances before and after the UPFC, respectively; v is the generator terminal voltage and v_b is the infinite bus voltage. The nominal parameters of the case study power system are given in the Appendix.

3.1 UPFC MATHEMATICA NONLINEAR MODEL

In order to study dynamic nature of UPFC, it needs to be modeled dynamically. Using Park's transformation and disregarding the resistance and transients of the ET and BT transformers, the non-linear dynamic model of the system installed with UPFC is given as [4, 5]:

$$\begin{bmatrix} v_{Etd} \\ v_{Etq} \end{bmatrix} = \begin{bmatrix} 0 & -x_E \\ x_E & 0 \end{bmatrix} \begin{bmatrix} i_{Ed} \\ i_{Eq} \end{bmatrix} + \begin{bmatrix} \frac{m_E cos\delta_E v_{dc}}{2} \\ \frac{m_E sin\delta_E v_{dc}}{2} \end{bmatrix} \tag{1}$$

$$\begin{bmatrix} v_{Btd} \\ v_{Btq} \end{bmatrix} = \begin{bmatrix} 0 & -x_B \\ x_B & 0 \end{bmatrix} \begin{bmatrix} i_{Bd} \\ i_{Bq} \end{bmatrix} + \begin{bmatrix} \frac{m_B cos\delta_B v_{dc}}{2} \\ \frac{m_B sin\delta_B v_{dc}}{2} \end{bmatrix} \tag{2}$$

$$\dot{v}_{dc} = \frac{3m_E}{4C_{dc}} \begin{bmatrix} cos\delta_E & sin\delta_E \end{bmatrix} \begin{bmatrix} i_{Ed} \\ i_{Eq} \end{bmatrix} + \frac{3m_B}{4C_{dc}} \begin{bmatrix} cos\delta_B & sin\delta_B \end{bmatrix} \begin{bmatrix} i_{Bd} \\ i_{Bq} \end{bmatrix} \tag{3}$$

where v_{Et}, i_E, v_{Bt}, and i_B are the excitation voltage, excitation current, boosting voltage, and boosting current, respectively, in which d and q subscripts stand for dq reference frame; C_{dc} and v_{dc} are the DC link capacitance and voltage, respectively. The current equations of excitation and boosting transformers can be written as:

$$i_{Ed} = \frac{x_{BB}}{x_{d\Sigma}} E_q^{'} - \frac{x_{Bd}}{2x_{d\Sigma}} m_E v_{dc} sin\delta_E + \frac{x_{dE}}{x_{d\Sigma}} \left(v_b cos\delta + \frac{1}{2} m_B v_{dc} sin\delta_B \right) \tag{4}$$

$$i_{Eq} = \frac{x_{Bq}}{2x_{q\Sigma}} m_E v_{dc} cos\delta_E - \frac{x_{qE}}{x_{q\Sigma}} \left(v_b sin\delta + \frac{1}{2} m_B v_{dc} cos\delta_B \right) \tag{5}$$

$$i_{Bd} = \frac{x_E}{x_{d\Sigma}} E_q^{'} + \frac{x_{dE}}{2x_{d\Sigma}} m_E v_{dc} sin\delta_E - \frac{x_{dt}}{x_{d\Sigma}} \left(v_b cos\delta + \frac{1}{2} m_B v_{dc} sin\delta_B \right) \tag{6}$$

$$i_{Bq} = -\frac{x_{qE}}{2x_{q\Sigma}} m_E v_{dc} cos\delta_E + \frac{x_{qt}}{x_{q\Sigma}} \left(v_b sin\delta + \frac{1}{2} m_B v_{dc} cos\delta_B \right) \tag{7}$$

where

$x_{BB} = x_B + x_{sb}$
$x_{dE} = x_d^{'} + x_{tE} + x_{ts}$
$x_{qE} = x_q + x_{tE} + x_{ts}$
$x_{d\Sigma} = x_{BB}\left(x_E + x_{d\Sigma}\right) + x_E x_{dE}$
$x_{q\Sigma} = x_{BB}\left(x_E + x_{q\Sigma}\right) + x_E x_{qE}$
$x_{Bd} = x_{BB} + x_{dE}$
$x_{Bq} = x_{BB} + x_{qE}$
$x_{dt} = x_E + x_{dE}$
$x_{qt} = x_E + x_{qE}$

where x_E and x_B are the ET and BT reactances, respectively. The non-linear model of the SMIB system of Fig. 1 is:

$$\dot{\delta} = \omega_b \left(\omega - 1\right) \tag{8}$$

$$\dot{\omega} = \frac{1}{M} \left(P_m - P_e - D\left(\omega - 1\right)\right) \tag{9}$$

$$\dot{E}_q^{'} = \frac{1}{T_{d0}^{'}} \left(E_{fd} - E_q\right) \tag{10}$$

$$\dot{E}_{fd} = \frac{1}{T_A} \left(k_A \left(v_{ref} - v\right) - E_{fd}\right) \tag{11}$$

where

$P_e = v_d i_d + v_q i_q$

$i_d = i_{Ed} + i_{Bd}$, $i_q = i_{Eq} + i_{Bq}$

$v_d = x_q i_q$, $v_q = E_q^{'} - x_d^{'} i_d$

$E_q = \left(x_d - x_d^{'}\right) i_d + E_q^{'}$

$v = \sqrt{{v_d}^2 + {v_q}^2}$

where P_m and P_e are the input and output power, respectively; M and D the inertia fixed and damping coefficient, respectively; ω_b the synchronous speed; δ and ω the rotor angle and speed, respectively; $E_q^{'}$,

E'_{fd}, and v the generator internal, field and terminal voltages, respectively; T'_{d0} the open circuit field time constant; x_d, x'_d, and x_q the d-axis reactance, d-axis transient reactance, and q-axis reactance, respectively; k_A and T_A the exciter gain and time constant, respectively; and v_{ref} the reference voltage.

3.2 LINEARIZED MODEL OF THE SYSTEM

The non-linear dynamic equations can be linearized around an operating point condition. The linearized model of power system as shown in Fig. 1 is explained by:

$$\Delta\dot{\delta} = \omega_b \Delta\omega \tag{12}$$

$$\Delta\dot{\omega} = -\frac{1}{M}\left(\Delta P_e + D\Delta\omega - \Delta P_m\right) \tag{13}$$

$$\Delta\dot{E}'_q = \frac{1}{T'_{d0}}\left(\Delta E_{fd} - \Delta E_q\right) \tag{14}$$

$$\Delta\dot{E}_{fd} = -\frac{1}{T_A}(\Delta E_{fd} + k_A \Delta v) \tag{15}$$

$$\begin{aligned}\Delta\dot{v}_{dc} =& k_7\Delta\delta + k_8\Delta E'_q + k_9\Delta v_{dc} + k_{ce}\Delta m_E + \\ & k_{c\delta e}\Delta\delta_E + k_{cb}\Delta m_B + k_{c\delta b}\Delta\delta_B\end{aligned} \tag{16}$$

where

$\Delta P_e = k_1\Delta\delta + k_2\Delta E'_q + k_{pd}\Delta v_{dc} + k_{pe}\Delta m_E + k_{p\delta e}\Delta\delta_E + k_{pb}\Delta m_B + k_{p\delta b}\Delta\delta_B$

$\Delta E_q = k_4\Delta\delta + k_3\Delta E'_q + k_{qd}\Delta v_{dc} + k_{qe}\Delta m_E + k_{q\delta e}\Delta\delta_E + k_{qb}\Delta m_B + k_{q\delta b}\Delta\delta_B$

$\Delta v = k_5\Delta\delta + k_6\Delta E'_q + k_{vd}\Delta v_{dc} + k_{ve}\Delta m_E + k_{v\delta e}\Delta\delta_E + k_{vb}\Delta m_B + k_{v\delta b}\Delta\delta_B$

In state-space representation, the power system can be modeled as:

$$\dot{x} = Ax + Bu \tag{17}$$

where the state vector x, control vector u, state matrix A and input matrix B are:

$$x = [\ \Delta\delta \quad \Delta\omega \quad \Delta E'_q \quad \Delta E_{fd} \quad \Delta v_{dc}\ ]^T$$

$$u = [\ \Delta v_{ref} \quad \Delta P_m \quad \Delta m_E \quad \Delta\delta_E \quad \Delta m_B \quad \Delta\delta_B\ ]^T$$

$$A = \begin{bmatrix} 0 & \omega_b & 0 & 0 & 0 \\ -\frac{k_1}{M} & -\frac{D}{M} & -\frac{k_2}{M} & 0 & -\frac{k_{pd}}{M} \\ -\frac{k_4}{T'_{d0}} & 0 & -\frac{k_3}{T'_{d0}} & \frac{1}{T'_{d0}} & -\frac{k_{qd}}{T'_{d0}} \\ -\frac{k_A k_5}{T_A} & 0 & -\frac{k_A k_6}{T_A} & -\frac{1}{T_A} & -\frac{k_A k_{vd}}{T_A} \\ k_7 & 0 & k_8 & 0 & k_9 \end{bmatrix}$$

$$B = \begin{bmatrix} 0 & 0 & 0 & 0 & 0 & 0 \\ 0 & \frac{1}{M} & -\frac{k_{pe}}{M} & -\frac{k_{p\delta e}}{M} & -\frac{k_{pb}}{M} & -\frac{k_{p\delta b}}{M} \\ 0 & 0 & -\frac{k_{qe}}{T'_{d0}} & -\frac{k_{q\delta e}}{T'_{d0}} & -\frac{k_{qb}}{T'_{d0}} & -\frac{k_{q\delta b}}{T'_{d0}} \\ \frac{K_A}{T_A} & 0 & -\frac{k_A k_{ve}}{T_A} & -\frac{k_A k_{v\delta e}}{T_A} & -\frac{k_A k_{vb}}{T_A} & -\frac{k_A k_{v\delta b}}{T_A} \\ 0 & 0 & k_{ce} & k_{c\delta e} & k_{cb} & k_{c\delta b} \end{bmatrix}$$

The linearized dynamic model of the state-space representation is shown in Fig. 2.

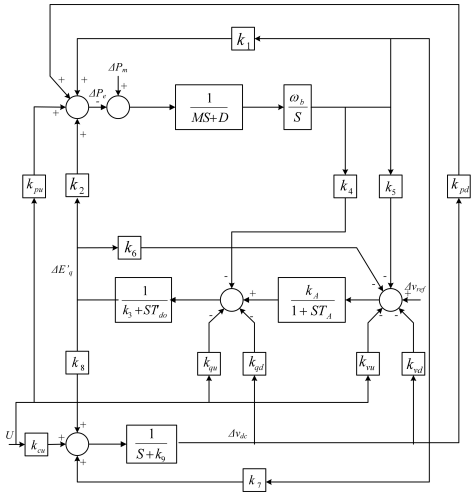

Fig.2: *Modified Phillips-Heffron transfer function model with UPFC [5].*

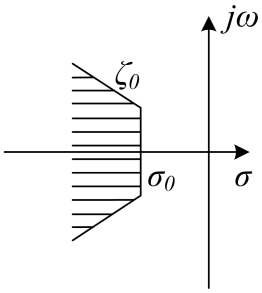

Fig.3: *S-plane representation of objective function.*

4. METHODOLOGY TO ENHANCE LFO DAMPING CAPABILITY

4.1 OPTIMAL SITING OF UPFC ON A TRANSMISSION LINE

In order to find the optimal place of UPFC on the transmission line, we used an eigenvalue-based objective function. The objective function is a combination of damping factor and damping ratio (Fig. 3) as follows:

$$J = \sum_j \left(\sum_{\sigma_i \geq \sigma_0} (\sigma_0 - \sigma_i)^2 + a \sum_{\zeta_i \leq \zeta_0} (\zeta_0 - \zeta_i)^2 \right) \tag{18}$$

where σ_i and ζ_i are the real part and the damping ratio of the i-th eigenvalue, respectively and j is the counter for the operating conditions. In this paper four operating conditions are considered which are given in the Appendix. Small steps are taken and objective function is computed. In this paper, a, σ_0 and ζ_0 are chosen as 10, -2 and 0.5, respectively based on [7]. We considered the line length as 1 pu and calculated the objective function for small steps on the transmission line in four different loading conditions. For each loading condition, we obtained a curve as in Fig. 4 that represents the lowest and highest costs for UPFC location. In order to compromise among the

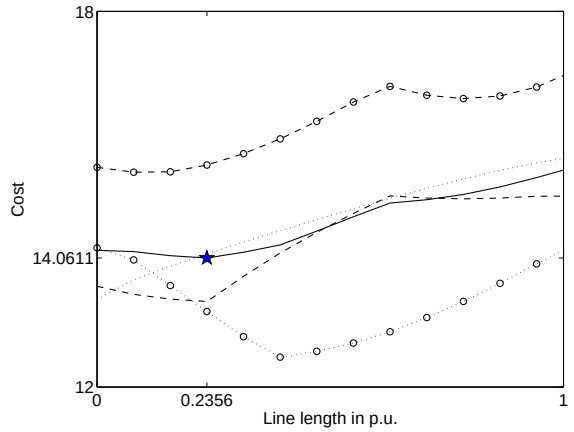

Fig.4: *Optimal place of UPFC on a transmission line: solid (average of all loading conditions), dotted with circles (nominal loading), dotted (light loading), dashed with circles (heavy loading) and dashed (leading power factor loading).*

results for each loading condition, we calculated the average of all loading conditions which can be seen as a solid line on the figure. From the solid line, the optimal location of UPFC, in terms of small signal stability, is 0.2356 pu. (from the figure it is obvious that end of line is not a good place to install the UPFC.)

4.2 ICA-BASED UPFC SUPPLEMENTARY CONTROLLER

4.2.1 IMPERIALIST COMPETITIVE ALGORITHM

ICA is a recently developed evolutionary optimization method which is inspired by imperialistic competition [20]. Like other evolutionary algorithms such as PSO, GA, COA, etc., it starts with an initial population which is called country and is divided into two types of colonies and imperialists which together form empires. Imperialistic competition among these empires forms the proposed evolutionary optimization algorithm. During this competition, weak empires collapse and powerful ones take possession of their colonies. Imperialistic competition converges to a state in which there exists only one empire and colonies have the same cost function value as the imperialist. After dividing all colonies among imperialists and creating the initial empires, these colonies start moving toward their related imperialist state which is called assimilation policy. The pseudo code of imperialist competitive algorithm is as follow [20]:

1. Select some random points on the function and initialize the empires.
2. Move the colonies toward their relevant imperialist (Assimilation).
3. Randomly change the position of some colonies (Revolution).

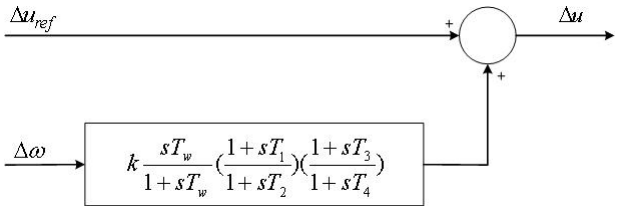

Fig.5: *Lead-lag supplementary controller of UPFC.*

4. If there is a colony in an empire which has lower cost than the imperialist, exchange the positions of that colony and the imperialist.
5. Unite the similar empires.
6. Compute the total cost of all empires.
7. Pick the weakest colony (colonies) from the weakest empires and give it (them) to one of the empires (Imperialistic competition).
8. Eliminate the powerless empires.
9. If stop conditions satisfied, stop, if not go to 2.

4.2.2 UPFC SUPPLEMENTARY CONTROLLER DESIGN

A UPFC damping controller is provided to improve the damping of power system oscillations. Fig. 5 shows the structure of UPFC controller. It comprises a gain block, signal-washout block and lead-lag compensators [1]. The speed deviation $\Delta\omega$ is considered as the input to the damping controller. Values of controller parameters should be kept within specified limits. In this paper, ICA is used for the optimal computation of controller parameters. It is necessary to mention here that only the unstable or lightly damped electromechanical modes of oscillations are relocated. The design problem can be formulated as the following constrained optimization problem, where the constraints are the bounds of controller parameters:

Minimize objective function for the UPFC controller subject to

$$\begin{aligned} k^{min} &\le k \le k^{max} \\ {T_1}^{min} &\le T_1 \le {T_1}^{max} \\ {T_2}^{min} &\le T_2 \le {T_2}^{max} \\ {T_3}^{min} &\le T_3 \le {T_3}^{max} \\ {T_4}^{min} &\le T_4 \le {T_4}^{max} \end{aligned} \tag{19}$$

Typical ranges of the optimized parameters of lead-lag controller are [-100, 100] for k, [0.05, 1.5] for T_1, T_2, T_3 and T_4.

5. SIMULATION RESULTS

5.1 ICA-BASED UPFC SUPPLEMENTARY CONTROLLER

ICA algorithm is used to solve optimization problem and search for an optimal or near optimal set of

Table 1: *Optimal parameters of the ICA-based controller.*

	k	T_1	T_2	T_3	T_4
UPFC on the sending bus	-8.6867	0.0500	0.4458	0.5614	0.0500
UPFC on the optimal place	-6.9809	0.0500	0.0500	0.0500	0.0500

UPFC-based controller parameters. Based on singular value decomposition (SVD) analysis in [1] modulating δ_E has an excellent capability in damping low frequency oscillations in comparison with other inputs of UPFC, thus in this paper, δ_E is modulated in the damping controller. Table 1 shows the optimal controller parameters, when UPFC is installed on the sending bus and on the proposed optimal place considering LFO damping.

5.2 EIGENVALUE ANALYSIS

The eigenvalues and damping ratios of electromechanical modes with and without ICA-based UPFC controller on the sending bus and on the optimal place at three different loading conditions are given in Table 2. The bold face numbers are the damping ratios related to electromechnical eigenvalues. The results show that installing UPFC on the optimal place and using supplementary controller improve overall system stability by moving the eigenvlaues to near σ_0 in s-plane.

5.3 TIME DOMAIN SIMULATION

The system behavior has been tested, applying 10% step increase in mechanical power input at t=1s. The dynamic responses for $\Delta\delta$ and $\Delta\omega$ under three different loading conditions, with and without δ_E based controller on the sending bus as well as optimal place are shown in Figs. 6 and 7. The dynamic response of δ_E is given in Fig. 8. It is obvious that the open loop system response, i.e. without controller, is unstable for all the loading conditions other than nominal condition, but when UPFC is installed on the optimal place, even with the lack of controller, responses are stable. The results clearly reveal that the system response to the disturbance is superior when it is installed on the proposed optimal place.

6. CONCLUSION

Up to now, researchers have studied damping capability of UPFC installing it on the sending bus of a transmission line. According to this issue, this paper suggested a new method to find the optimal place of UPFC controller on a transmission line. The effectiveness of the proposed method for damping of LFO was tested on a SMIB subjected to a disturbance, an increase in mechanical power input. Installation of UPFC on the sending bus and optimal place of transmission line were compared to each other and the results from eigenvalue analysis and time domain simulations confirm that the low frequency oscillations can be improved placing the UPFC on the proposed optimal location. The work conducted in this paper can be further improved studying UPFC allocation on multi-machine systems considering every step parts of all transmission lines.

7. APPENDIX

The system parameters and operating conditions are given as follow.

7.1 GENERATOR

M = 8.0 MJ/MVA. D = 0.0.
$T_{d0}^{'}$ =5.044 s. f = 60 Hz. v = 1.0 pu.
x_d = 1.2 pu. x_q = 1.2 pu. $x_d^{'}$ = 0.15 pu.
Nominal loading: P_e = 1.00 pu, Q_e = 0.015 pu.
Light loading: P_e = 0.30 pu, Q_e = 0.015 pu.
Heavy loading: P_e = 1.10 pu, Q_e = 0.400 pu.

7.2 EXCITATION SYSTEM

K_A = 20. T_A = 0.01 s.

7.3 TRANSFORMER

x_{tE} = 0.1 pu.

7.4 TRANSMISSION LINE

$x_{ts} + x_{sb}$ = 0.74 pu. v_b = 1.0.

7.5 UPFC

x_E = 0.1 pu. x_B = 0.1 pu. T_w = 5.0 s.
v_{dc} = 2 pu. C_{dc} = 1 pu.

References

[1] A. T. Al-Awami, Y. T. Abdel-Magid, and M. A. Abido, "A particle-swarm-based approach of power system stability enhancement with unified power flow controller," *Int. J. Elect. Power Energy Syst.*, vol. 29, no. 3, pp. 251-259, Mar. 2007.

[2] M. A. Abido, "Power system stability enhancement using FACTS controllers: A review," *Arab. J. Sci. Eng.*, vol. 34, no. 1B, pp. 153-172, Apr. 2009.

[3] L. Gyugyi, T. R. Rietman, A. Edris, C. D. Schauder, D. R. Torgerson, and S. L. Williams, "The unified power flow controller: A new approach to power transmission Control," *IEEE Trans. Power Del.*, vol. 10, no. 2, pp. 1085-1097, Apr. 1995.

Table 2: *System Eigenvalues and damping ratios with and without controller for three loading condition considering UPFC locations on a transmission line.*

	Nominal loading	Light loading	Heavy loading
without controller UPFC on send. bus	-98.5401 0.0140±j2.7609, **-0.0051** -1.2221±j1.0768, **0.7503**	-98.0427 0.3022±j2.7373, **-0.1338** -1.7605±j0.1103, **0.9980**	-98.3089 0.3338±j3.1149, **-0.1065** -0.7671 -2.5473
without controller UPFC on opt. bus	-98.1445 0.0660±j2.5115, **0.0263** -1.2135±j0.6483, **0.8820**	-97.5108 0.2146±j2.0613, **-0.1036** -2.7231 -0.9164	-97.8509 0.2043±j2.7638, **-0.0737** -2.7309 -0.5189
with controller UPFC on send. bus	-20.0000 -98.5459 -0.1984 -1.0787±j2.0157, **0.4718** -0.9038±j1.7561, **0.4576** -20.0000	-20.0000 -98.0447 -0.0006±j2.0269, **0.0003** -0.1983 -1.8873±j0.5760, **0.9565** -20.0000	-20.0000 -98.3144 -0.2443±j2.8951, **0.0841** -0.1981 -0.8779 -2.6126 -20.0000
with controller UPFC on opt. bus	-98.1522 -2.1730 -1.1614±j1.5433, **0.6013** -1.0101±j1.5253, **0.5521** -0.1975 -20.0000	-97.5124 -0.0890±j1.8210, **0.0488** -2.5889±j0.2511, **0.9953** -0.1986 -1.0820 -20.0000	-97.8585 0.3897±j2.4948, **0.1543** -0.1968 -0.5858 -2.5715±j0.1764, **0.9977** -20.0000

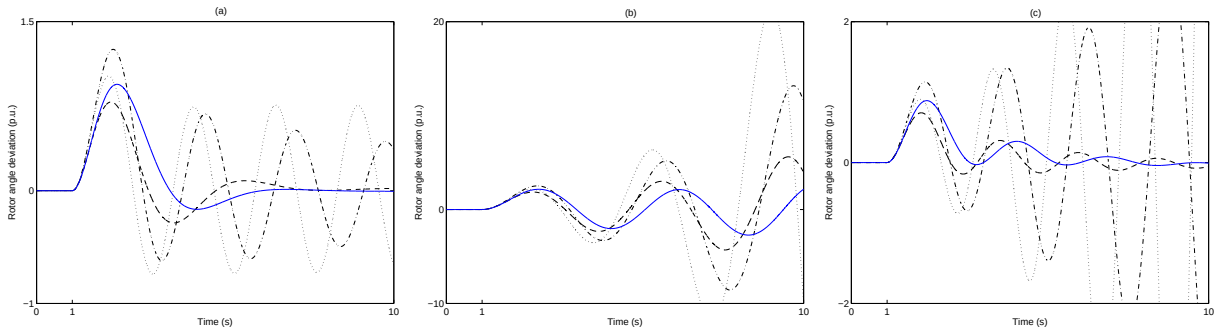

Fig.6: *Dynamic responses for $\Delta\delta$ at (a) Nominal (b) Light and (c) Heavy loading conditions: solid (with ICA-based UPFC controller on the optimal place), dashed (with ICA-based UPFC controller on the sending bus), dashed-dotted (without ICA-based UPFC controller on the optimal place) and dotted (without ICA-based UPFC controller on the sending bus).*

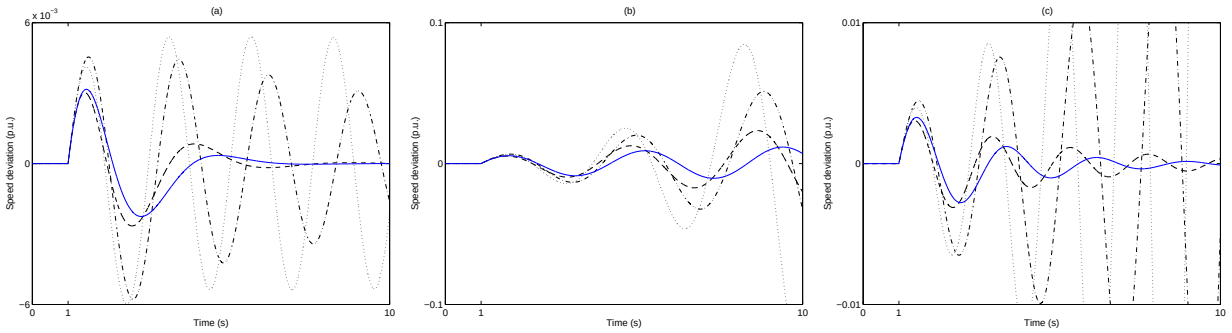

Fig.7: *Dynamic responses for $\Delta\omega$ at (a) Nominal (b) Light and (c) Heavy loading conditions: solid (with ICA-based UPFC controller on the optimal place), dashed (with ICA-based UPFC controller on the sending bus), dashed-dotted (without ICA-based UPFC controller on the optimal place) and dotted (without ICA-based UPFC controller on the sending bus).*

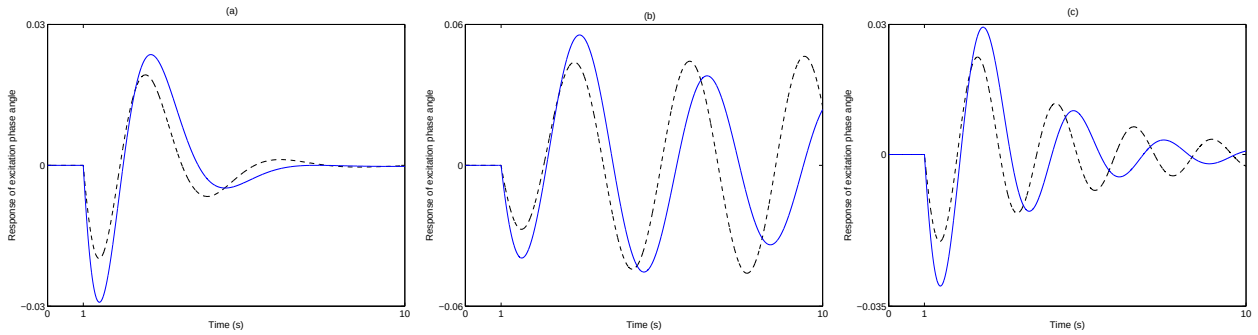

Fig.8: *Dynamic responses for $\Delta\delta_E$ at (a) Nominal (b) Light and (c) Heavy loading conditions: solid (with ICA-based UPFC controller on the optimal place), dashed (with ICA-based UPFC controller on the sending bus), dashed-dotted (without ICA-based UPFC controller on the optimal place) and dotted (without ICA-based UPFC controller on the sending bus).*

[4] A. Nabavi-Niaki, M. R. Iravani, "Steady-state and dynamic models of unified power flow controller (UPFC) for power system studies," *IEEE Trans. Power Syst.*, vol. 11, no. 4, pp. 1937-1943, Nov. 1996.

[5] H. F. Wang, "Damping function of unified power flow controller," *IEE Proc. Gener. Transm. Distrib.*, vol. 146, no. 1, pp. 81-87, Jan. 1999.

[6] H. F. Wang, "Applications of modelling UPFC into multi-machine power systems," *IEE Proc. Gener. Transm. Distrib.*, vol. 146, no. 3, pp. 306-312, May 1999.

[7] H. Shayeghi, H. A. Shayanfar, S. Jalilzadeh, and A. Safari, "A PSO based unified power flow controller for damping of power system oscillations," *Energy Conversion Manage.*, vol. 50, no. 10, pp. 2583-2592, Oct. 2009.

[8] B. Mohammadzadeh, R. Gholizadeh Roshanagh and S. Najafi Ravadanegh, "Optimal designing of SSSC based supplementary controller for LFO damping of power system using COA," *ECTI Trans. Electr. Eng., Electron. Commun.*, vol. 12, no. 2, pp. 64-72, Aug. 2014.

[9] M. R. Banaei, B. Mohammadzadeh and R. Reza Ahrabi, "Damping of low frequency electromechanical oscillations using UPFC based on cuckoo optimization algorithm," *Int. J. Electr. Eng. Informatics.*, vol. 6, no. 4, pp. 769-784, Dec. 2014.

[10] A. Ajami, R. Gholizadeh Roshanagh, "Optimal design of UPFC-based damping controller using imperialist competitive algorithm," *Turkish J. Electr. Eng. Comput. Sci.*, vol. 20, no. sup.1, pp. 1109-1122, Dec. 2012.

[11] K. D. V. N. Rao, S. Paul and T. K. Gangopadhyay, "Design of UPFC based damping controller for robust stabilization of power system low frequency oscillation using LMI technique," *Int. J. Eng. Sci. Adv. Technol.*, vol. 2, no. 2, pp. 338-345, Mar. 2012.

[12] A. Bekri and A. Hazzab, "ANFIS UPFC damping controller for multi machines power systems oscillations," *Przeglad Elektrotechniczny*, vol. 2013, no. 12, pp. 105-109, Dec. 2013.

[13] S. Gerbex, R. Cherkaou and A. J. Germond, "Optimal location of multi-type FACTS devices in a power system by means of genetic algorithms," *IEEE Trans. Power Syst.*, vol. 16, no. 3, pp. 537-544, Aug. 2001.

[14] F. G. M. Lima, F. D. Galiana, I. Kockar and J. Munoz, "Phase shifter placement in large-scale systems via mixed integer linear programming," *IEEE Trans. Power Syst.*, vol. 18, no. 3, pp. 1029-1034, Aug. 2003.

[15] J. Hao, L. B. Shi and C. Chen, "Optimising location of unified power flow controllers by means of improved evolutionary programming," *IEE Proc. Gener. Transm. Distrib.*, vol. 151, no. 6, pp. 705-712, Nov. 2004.

[16] A. K. Pradhan, A. Routray, and B. Mohanty,"Maximum efficiency of flexible AC transmission systems," *Int. J. Elect. Power Energy Syst.*, vol. 28, no. 8, pp. 581-588, Oct. 2006.

[17] P. R. Sharma, A. Kumar and N. Kumar, "Optimal location for shunt connected FACTS devices in a series compensated long transmission line," *Turkish J. Electr. Eng. Comput. Sci.*, vol. 15, no. 3, pp. 312-328, 2007.

[18] L. Ippolito and P. Siano, "Selection of optimal number and location of thyristor-controlled phase shifters using genetic based algorithms," *IEE Proc. Gener. Transm. Distrib.*, vol. 151, no. 5, pp. 630-637, Sep. 2004.

[19] N. K. Sharma, A. Ghosh and R. K. Varma, "A novel placement strategy for FACTS controllers," *IEEE Trans. Power Del.*, vol. 18, no. 3, pp. 982-987, Jul. 2003.

[20] E. Atashpaz-Gargari and C. Lucas, "Imperialist competitive algorithm: an algorithm for optimization inspired by imperialistic competition," *Proc. IEEE Congr. Evol. Comput. CEC 2007.*, 2007, pp. 4661-4667.

Reza Gholizadeh-Roshanagh obtained his B.Sc. degree (2008) from Islamic Azad University of Ardabil, Ardabil, Iran, and his M.Sc. degree (2011) from Azarbaijan Shahid Madani University (ASMU), Tabriz, Iran, both in Electrical Power Engineering. He is now a Ph.D. student of Electrical Power Engineering at ASMU.

Behrouz Mohammadzadeh obtained his B.Sc. degree (2010) from Islamic Azad University of Ardabil, Ardabil, Iran and his M.Sc. degree (2014) from Azarbaijan Shahid Madani University (ASMU), Tabriz, Iran, both in Electrical Power Engineering. He is now a Ph.D. student of Electrical Power Engineering at ASMU. He is also a member of Young and Elite Researchers Club, Islamic Azad University.

Sajad Najafi-Ravadanegh obtained his B.Sc. degree in Electrical Engineering from University of Tabriz, Iran in 2001 and M.Sc. and Ph.D. degrees in Electrical Engineering from Amirkabir University of Technology (AUT), Iran in 2003 and 2009 respectively. At the present, he is the assistant professor of Electrical Engineering department at Azarbaijan Shahid Madani University (ASMU). His research interests include Power System Stability and Control; Special Protection Schemes, Power System Controlled Islanding, FACTS Devices, Evolutionary Algorithms and Intelligent Computing in Power Systems, Distribution System Planning, Energy Management, Nonlinear Dynamic and Chaos. He is also author and co-author of over 40 technical papers.